Electronic Supporting Information:

Truxene based Porous, Crystalline Covalent Organic Frameworks and it's Applications in Humidity Sensing

Harpreet Singh,[1] Vijay K. Tomer,[2] Nityasagar Jena,[2] Indu Bala,[1] Nidhi Sharma,[2] Devadutta Nepak,[2] Abir De Sarkar*,[2] Kamalakannan Kailasam*[2], Santanu Kumar Pal*[1]

[1] Department of Chemical Sciences, Indian Institute of Science Education and Research (IISER) Mohali, Sector-81, SAS Nagar, Mohali 140306, India.
E-mail: skpal@iisermohali.ac.in

[2] Institute of Nano Science and Technology, Phase 10, Mohali 160062, India.
E-mail: abirdesarkar@gmail.com and kamal@inst.ac.in

Synthesis Scheme:

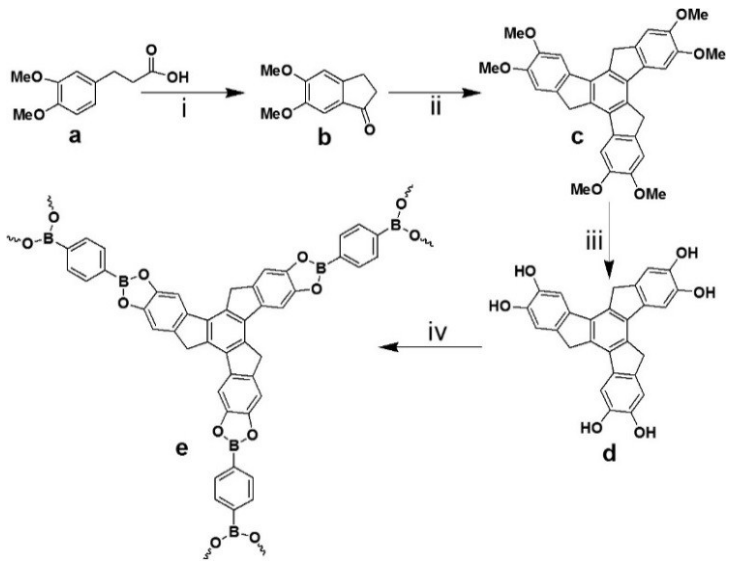

Scheme S1 Reaction conditions**:(i)** PPA, 110 °C **(ii)** PPE, 140 °C **(iii)** BBr_3, DCM **(iv)** 1,4 phenylenediboronic acid, dioxane/mesitylene/methanol (150:30:1), 110 °C.

Symmetric-COF-TXDBA (s-COF-TXDBA)

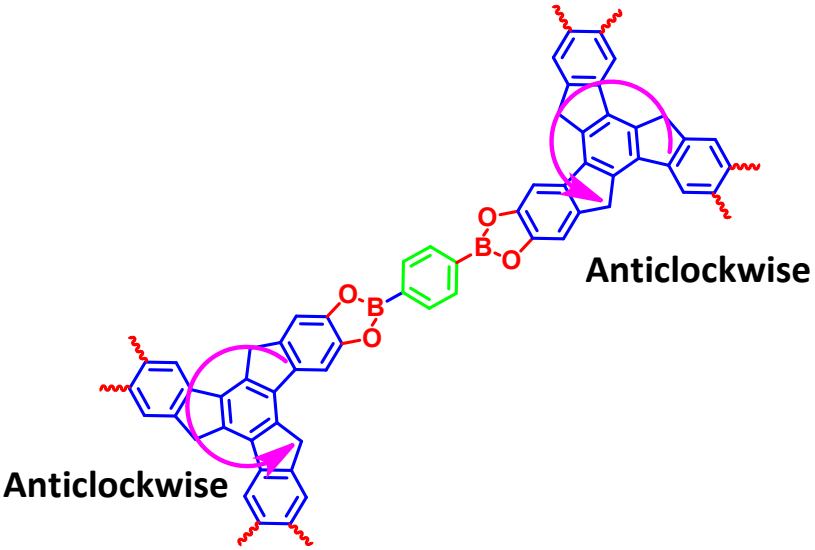

Asymmetric-COF-TXDBA (s-COF-TXDBA)

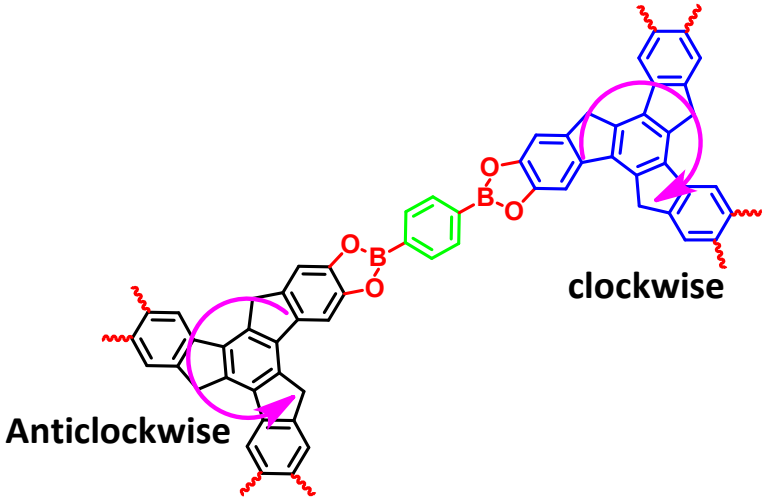

Scheme S2 Two possible structural arrangement of the precursors to build the periodic crystal lattices, Symmetric-COF-TXDBA (s-COF-TXDBA) and Asymmetric-COF-TXDBA (a-COF-TXDBA).

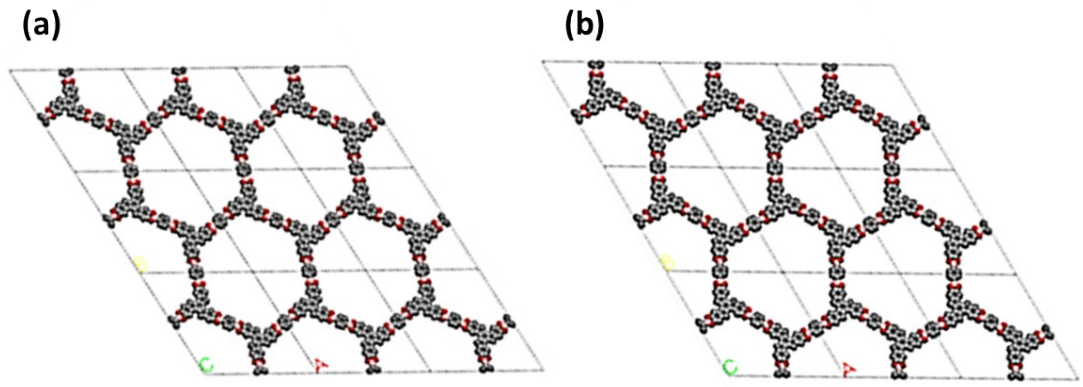

Scheme S3 (a) Symmetric-COF-TXDBA (s-COF-TXDBA) with symmetric honeycomb like pore produced by symmetric building block; (b) Asymmetric-COF-TXDBA (a-COF-TXDBA) with asymmetric pore shape produced by asymmetric building blocks.

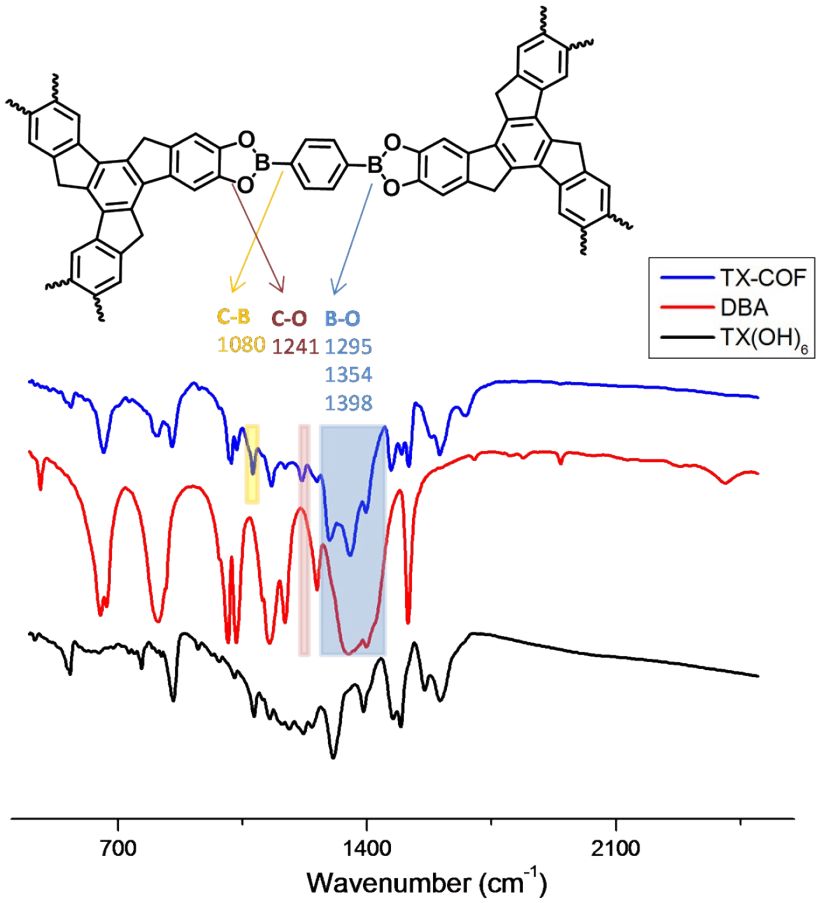

Fig. S1 The IR spectrum of COF-TXDBA (Blue); Compound (d) (Black); 1,4-phenylenediboronic acid (Red).

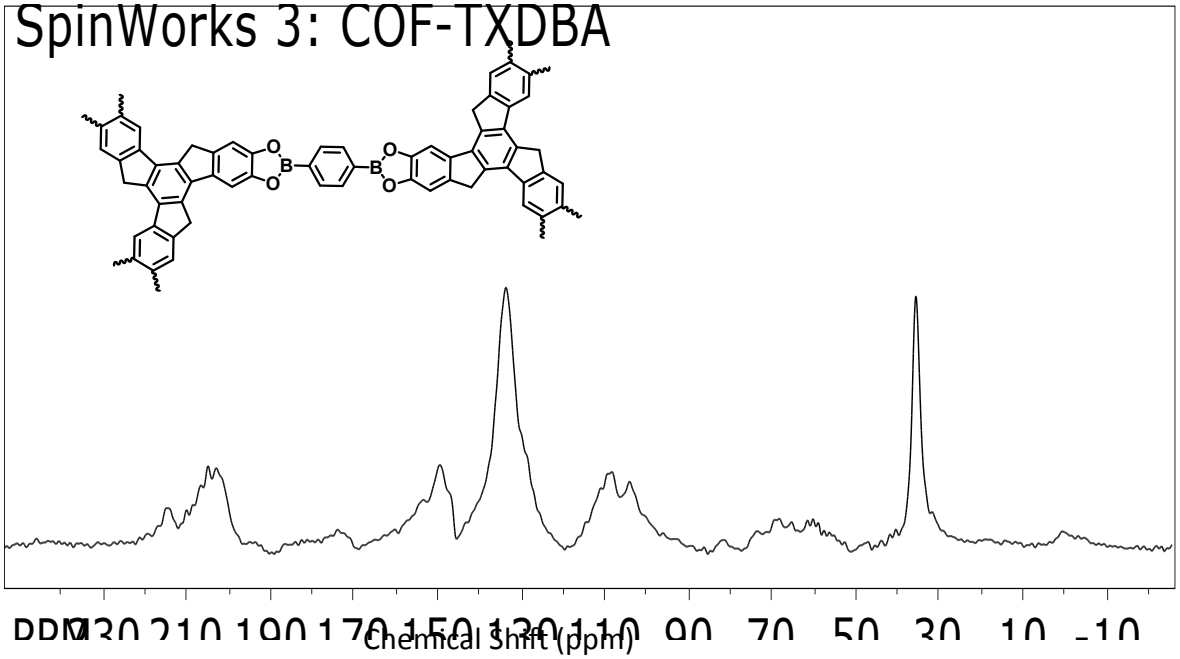

Fig. S2 | Solid state $^{13}C\{^{1}H\}$ CPMAS NMR of COF-TXDBA.

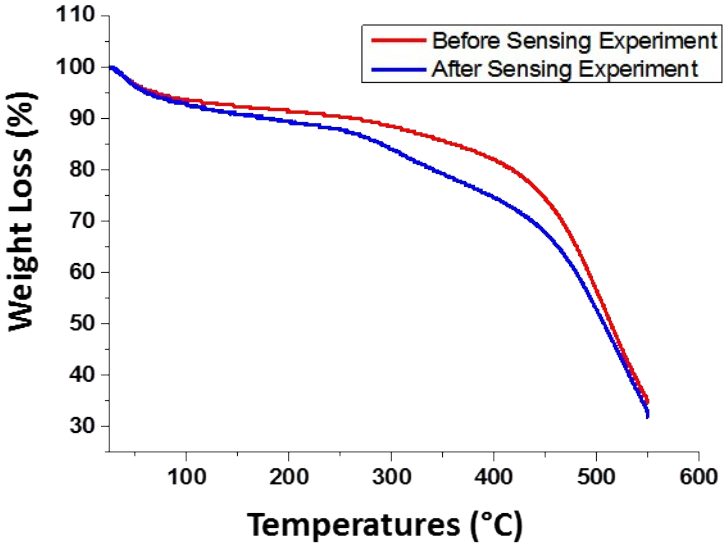

Fig. S3 | Thermogravimetric analyses (TGA) of as synthesized COF-TXDBA shows minimal weight loss upto 410 °C. The weight loss at lower temperatures < 200 °C is attributed to the evaporation of solvent molecules present in the nano-channels of COF-TXDBA. Further, TGA analysis of sample after the sensing experiment shows nearly 10% weight loss after 250 °C as compare to as synthesized COF-TXDBA, which can be attributed to formation of small amount of oligomers during interaction of water molecule and COF-TXDBA.

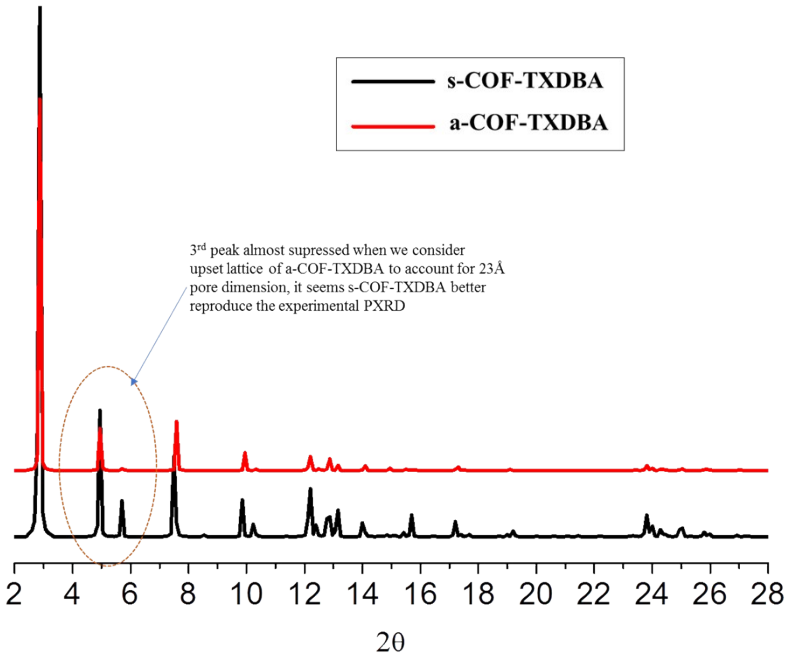

Fig.S4 Comparisons between simulated PXRD pattern of s-COF-TXDBA and a-COF-TXDBA shows appearance of sharp intense peaks at low angle regime for s-COF-TXDBA better reproduce the experimental PXRD.

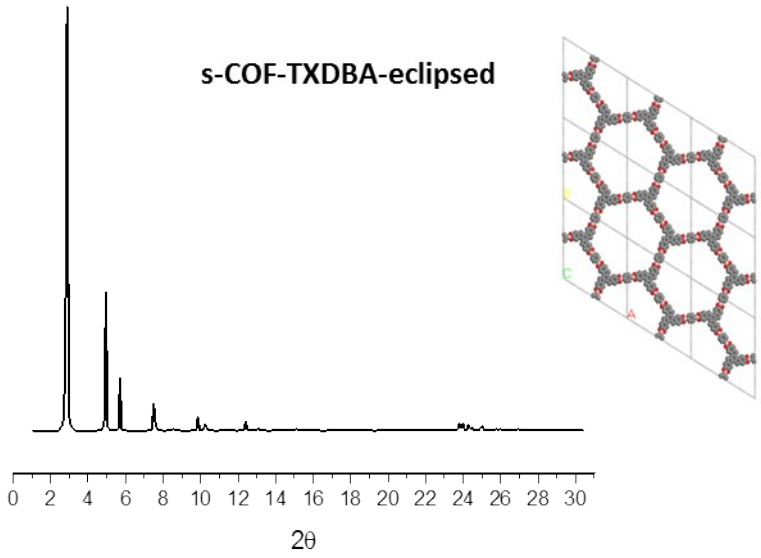

Fig.S5 Simulated PXRD of Symmetric-COF-TXDBA in eclipsed geometry (symmetric hexagonal pore).

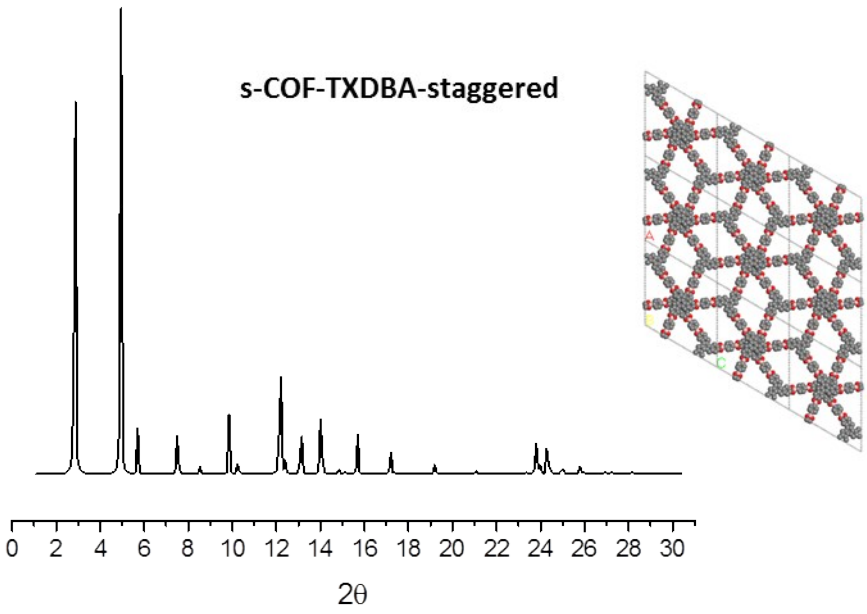

Fig.S6 | Simulated PXRD of Symmetric-COF-TXDBA in staggered geometry.

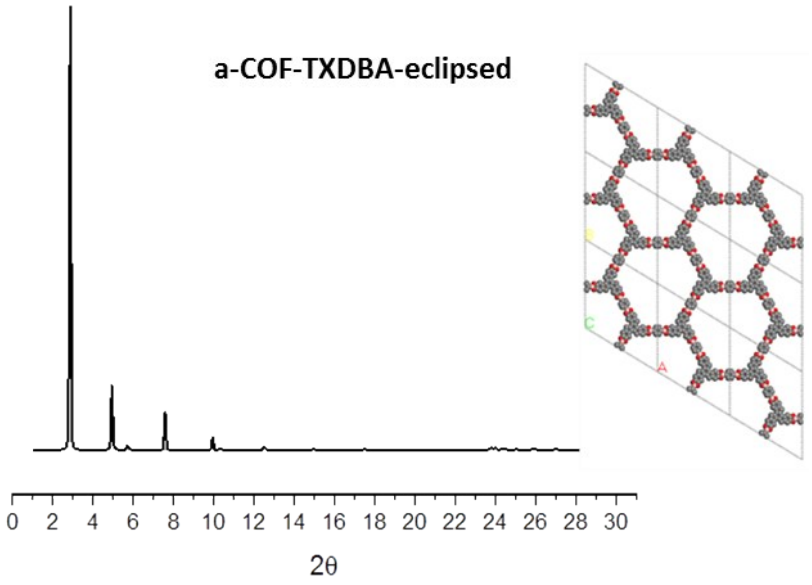

Fig.S7 | Simulated PXRD of Asymmetric-COF-TXDBA in eclipsed geometry (asymmetric hexagonal pore).

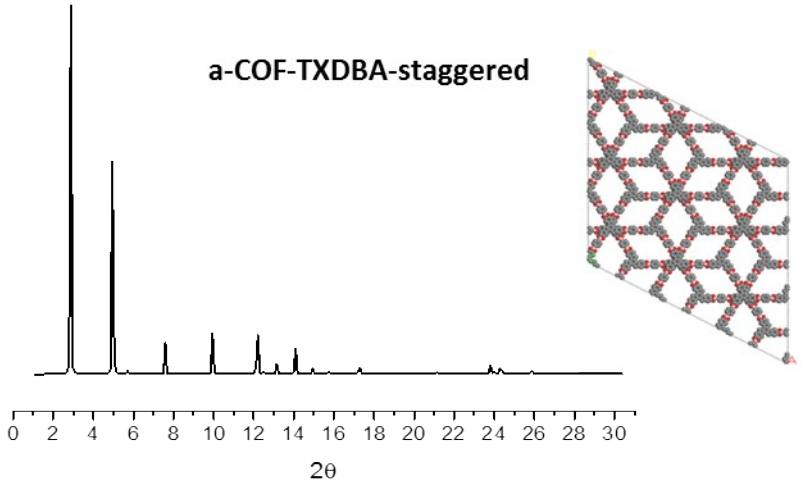

Fig.S8 | Simulated PXRD of Asymmetric-COF-TXDBA in staggered geometry.

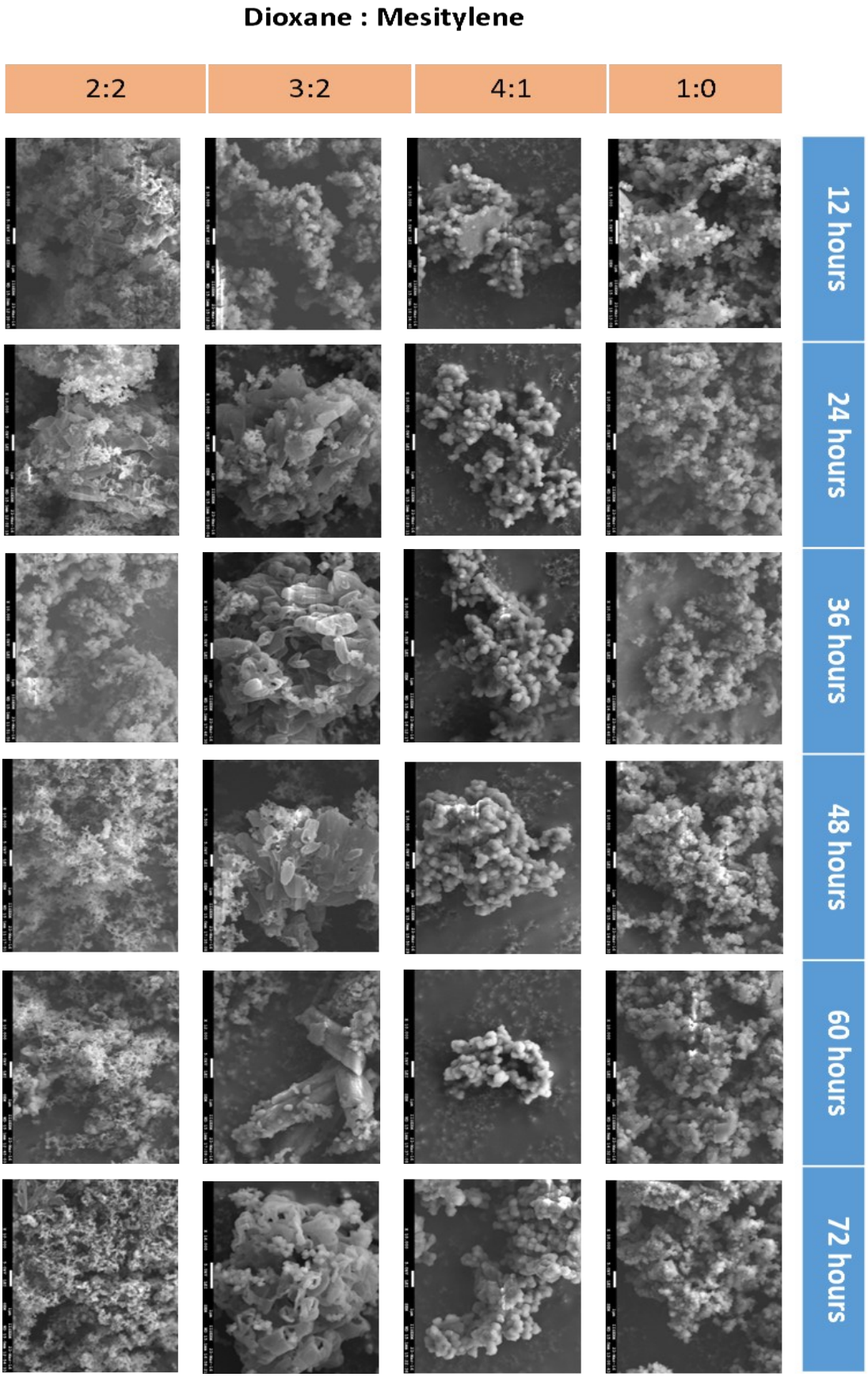

Fig. S9 | SEM images of Truxene COF at different Mesitylene and dioxane ratio at different times shows the formation of capsules at Dioxane: Mesitylene ratio 3:2.

^{1}H NMR spectra of compound (a).

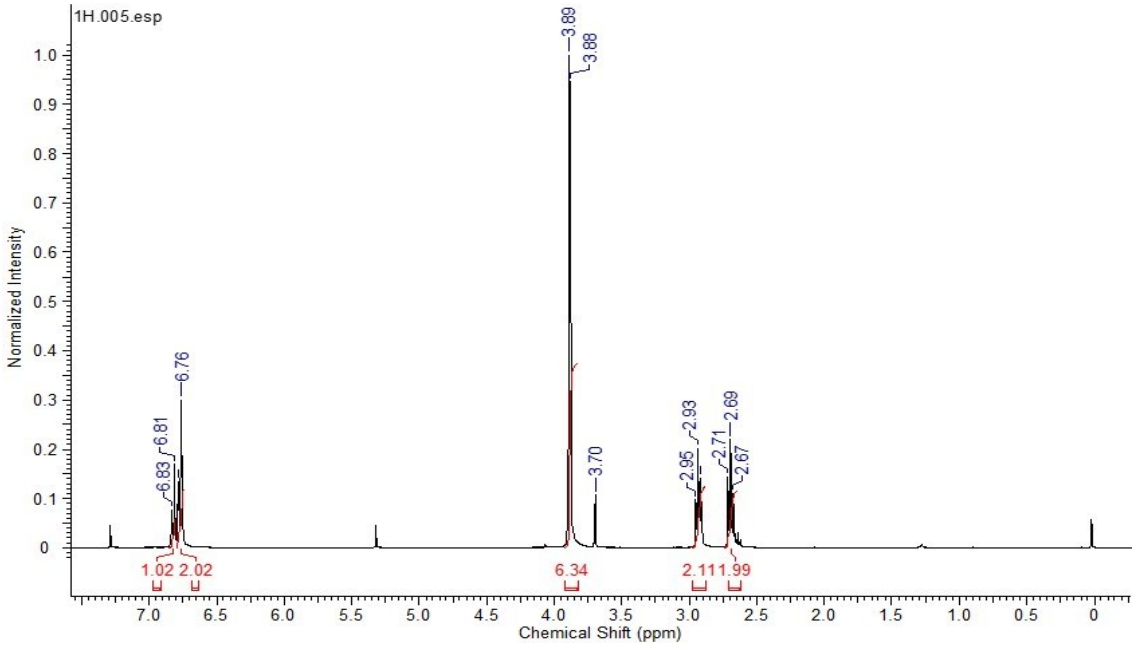

^{13}C NMR spectra of compound (a).

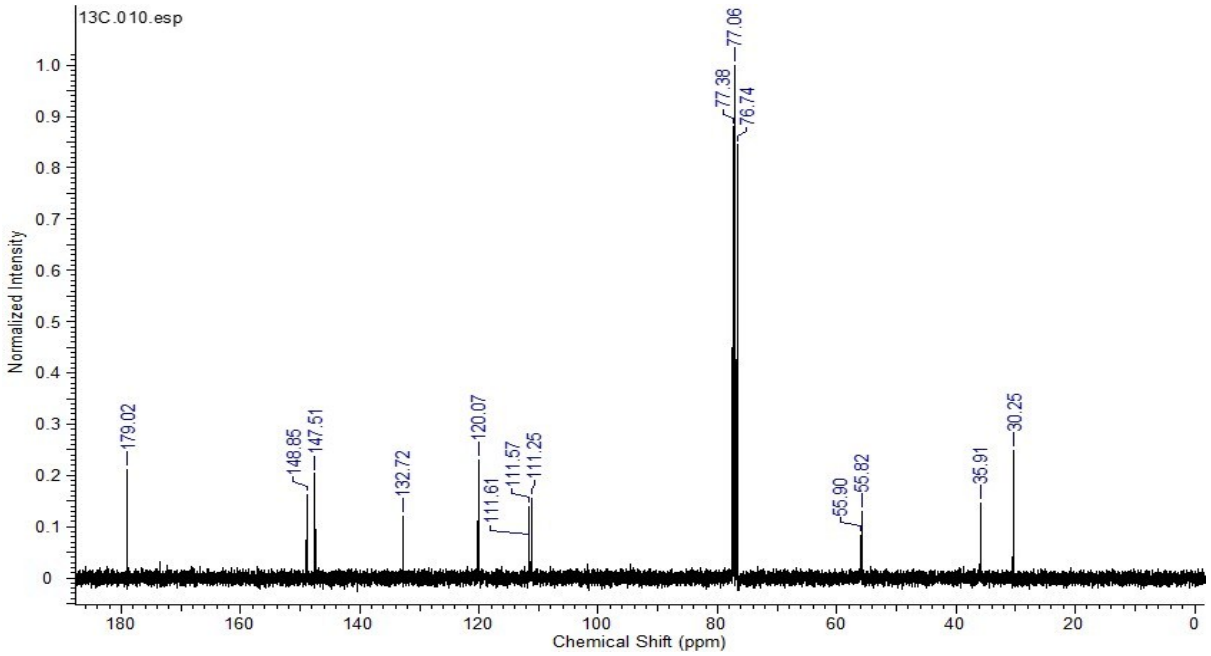

^{1}H NMR spectra of compound (b).

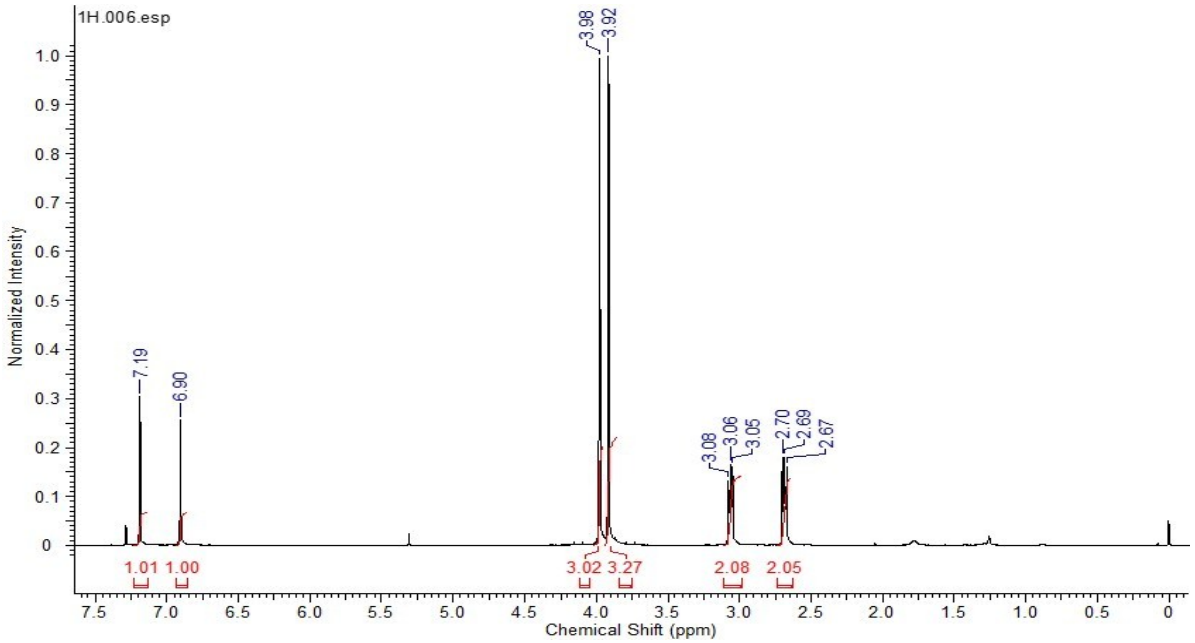

^{13}C NMR spectra of compound (b).

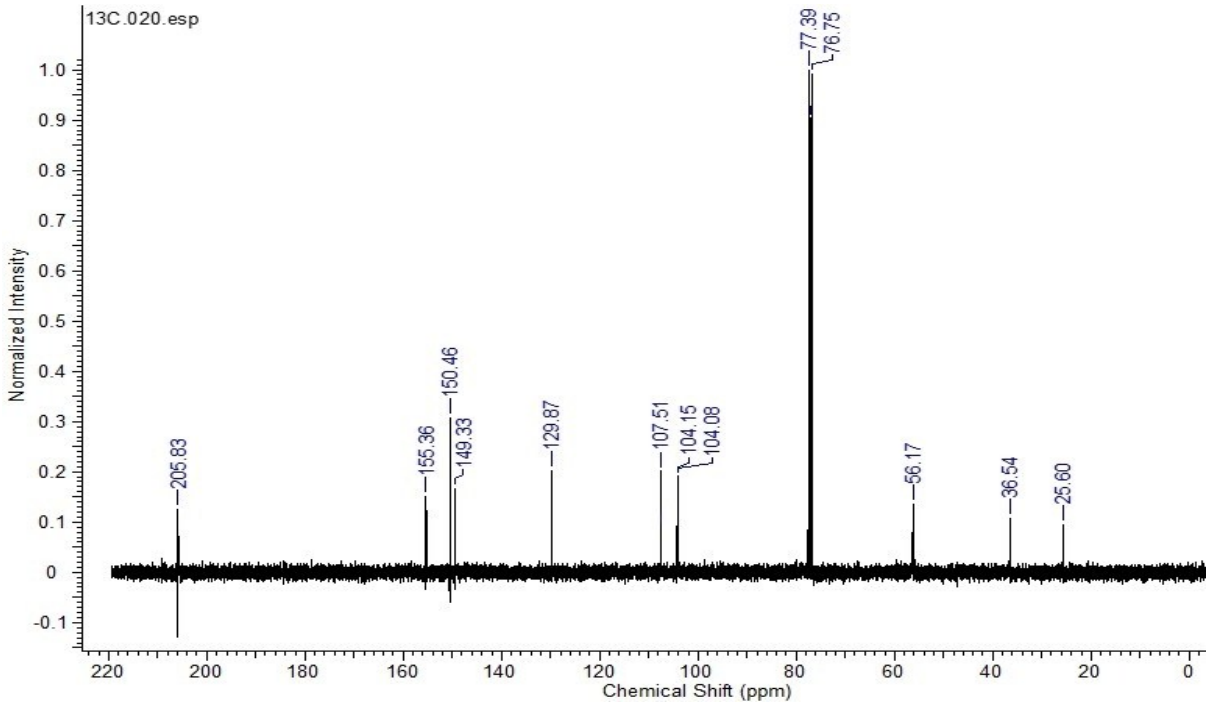

^{1}H NMR spectra of compound (d).

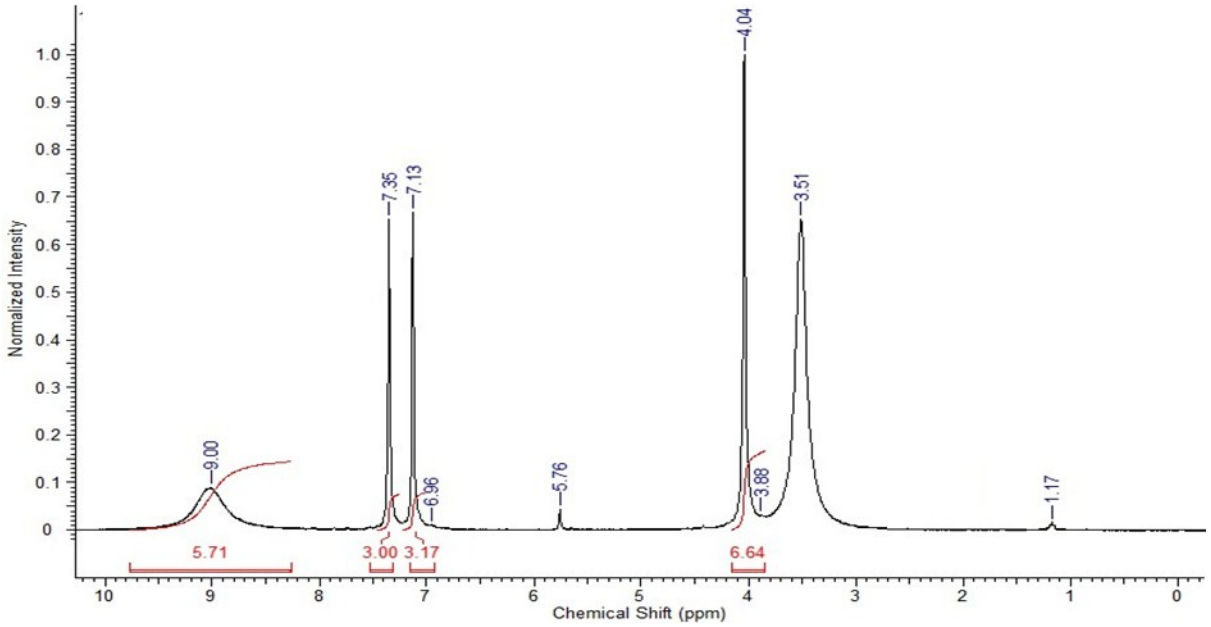

^{13}C NMR spectra of compound (d).

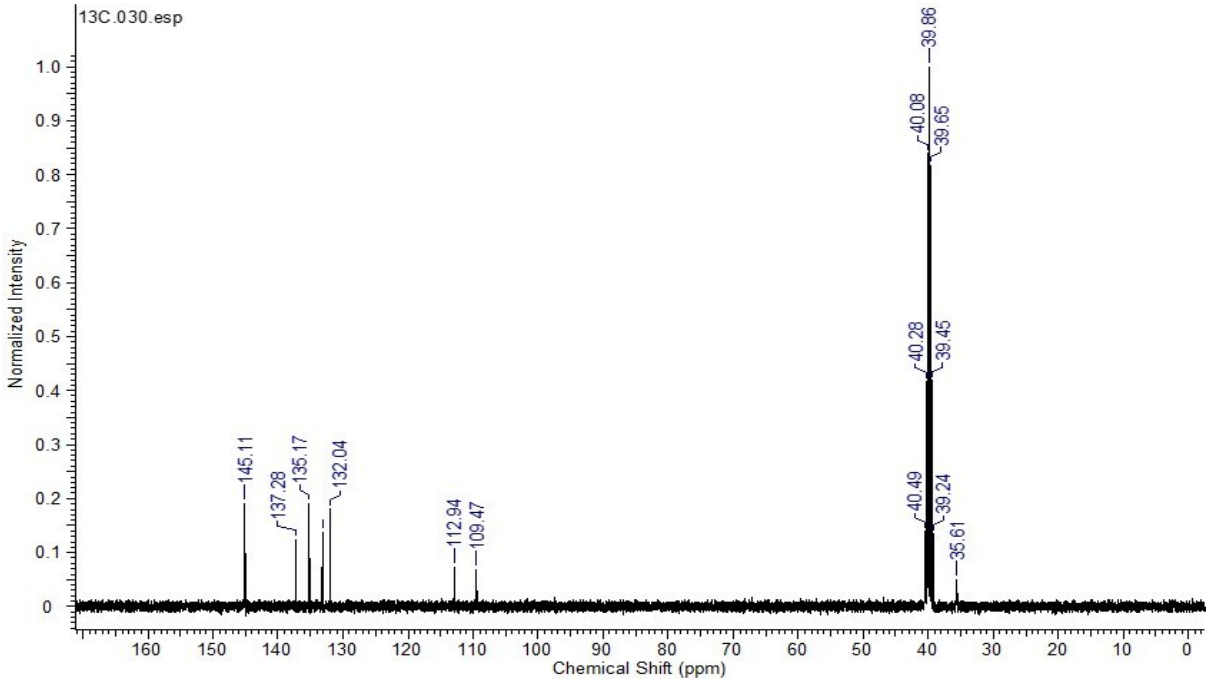

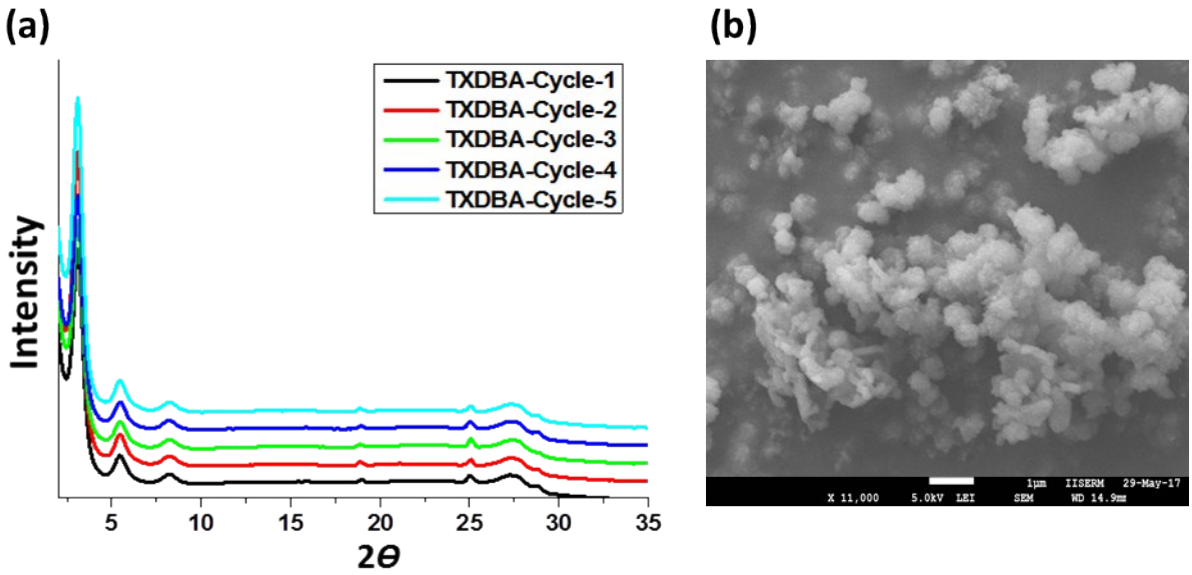

Fig S10: (a) %RH dependent stability test of COF-TXDBA is performed by checking its PXRD after each cycle of experiment from 11-98% RH. Sample was vacuum dried at 100 °C after each cycle. PXRD of COF shows that crystallinity of COF-TXDBA remains intact after five cycles of measurements; (b) SEM images of COF-TXDBA after fifth cycle of humidity sensing experiments.

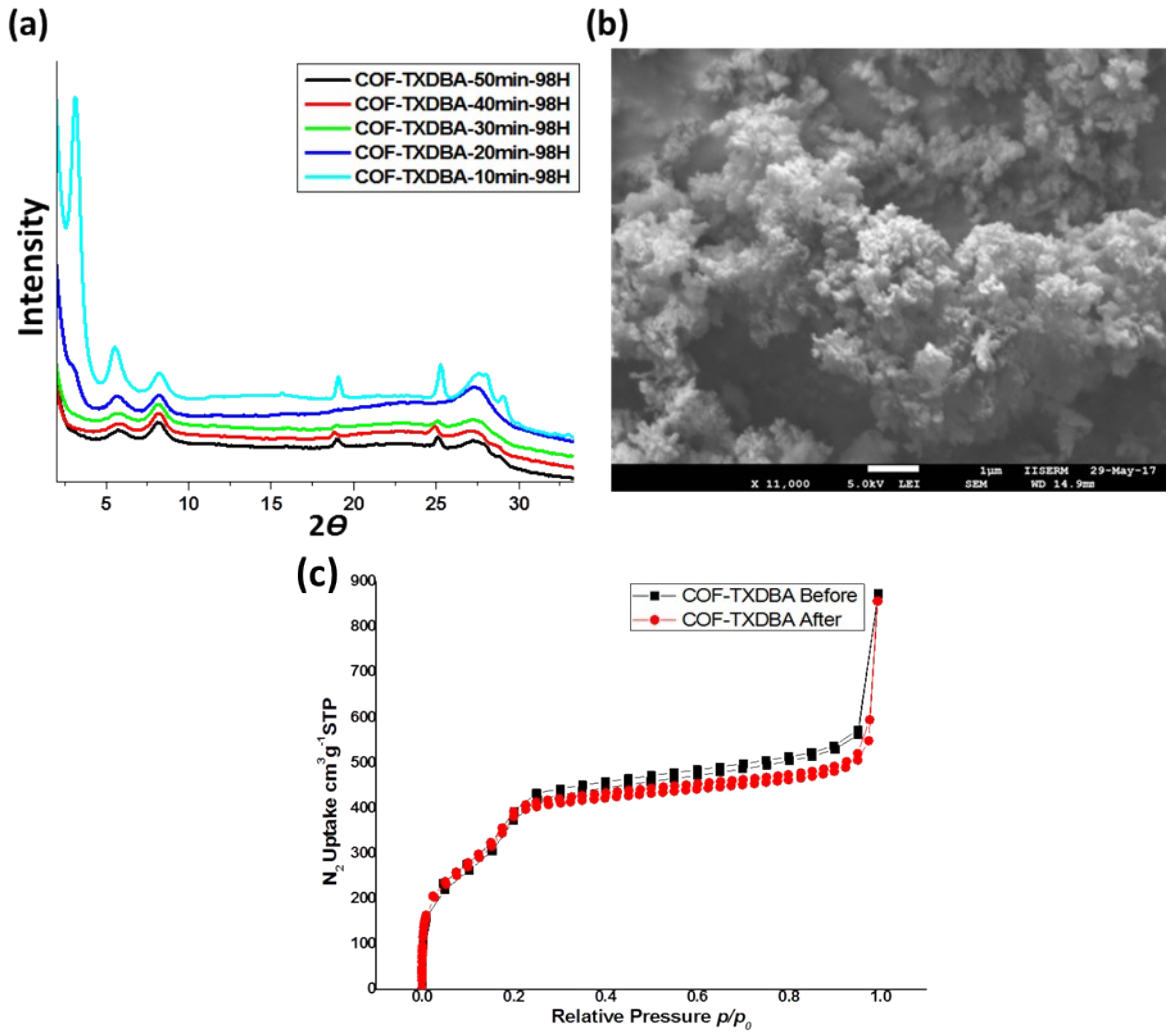

Fig S11: (a)Time-dependent stability test of COF-TXDBA by keeping the sample in 98% RH humidity chamber for 50 min. PXRD was measured after each 10 min intervals shows that long range order of COF-TXDBA reduces with time. (b) SEM images of COF-TXDBA after keeping the sample in 98% RH for long 50 min. (c) Nitrogen isotherm at 77 K for COF-TXDBA Before and After 98% RH for 50 min followed by overnight vacuum drying at 120 °C.

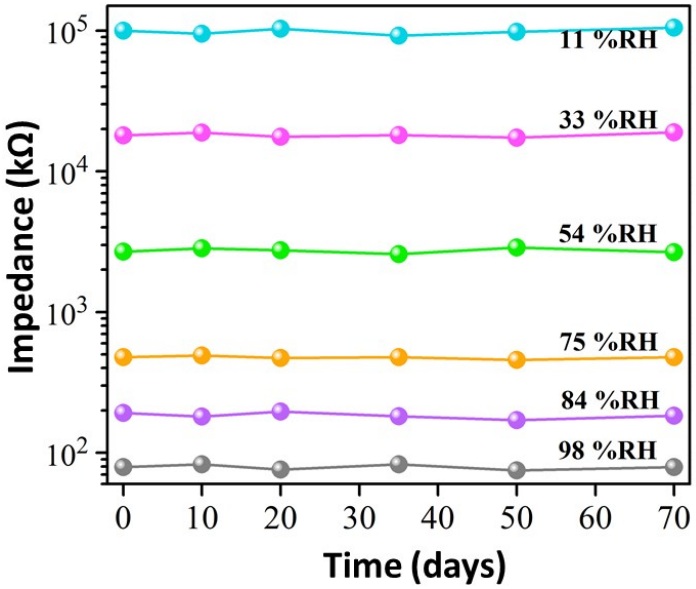

Fig S12: The response of COF-TXDBA monitored at different humidity conditions for 70 days.

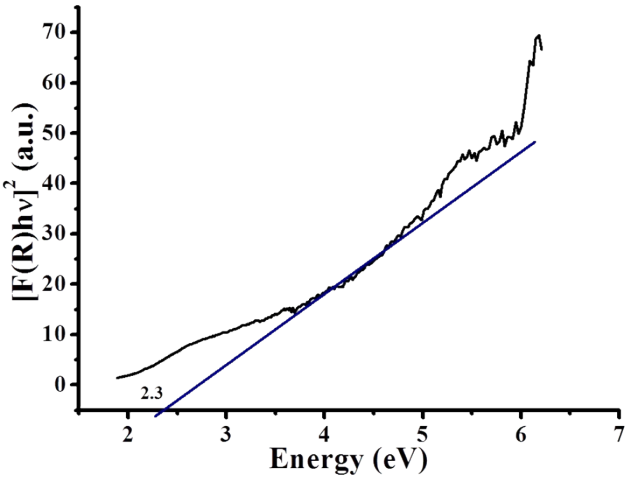

Fig. S13 Band gap measurement of COF-TXDBA.

Table T1: A comparison of humidity sensing performance of previously published works.

Sr. No.	Material	Order of magnitude change in impedance in complete %RH range	Response time (S)	Recovery time (S)	Hysteresis (%)	Ref
1	NiO-PPY/SBA-15	3.5	45	90	--	1
2	SnO_2/SBA-15	4.5	33	50	2.9	2
3	Fe/SiO_2	3.5	20	50	--	3
4	Li doped mesoporous silica	3	21	51	6	4
5	ZnO nanosheets	2	600	3	5	5
6	Feather like ZnO	2	40	80	--	6
7	ZnO cauliflowers	--	20	3	4.16	7
8	ZnO nanotetrapods	--	36	17	--	8
9	La^{3+} and K^+ doped TiO_2–10 mol% SnO_2	5	11	18	--	9
10	$SnWO_4$-SnO_2	3	30	100	--	10
11	K^+-doped SnO_2–$LiZnVO_4$	3	80	100	--	11
12	MgO-KCl/SiO_2	4	6	26	4	12
13	WO_3-SnO_2	3	117	411	3	13
14	NaCl-KIT-6	5	47	150	--	14
15	MCM-48 fiber	2	15	18	5	15
16	Fe/SnO_2	4	1	4	--	16
17	Nanoporous polymers based on 1,4-divinylbenzene	3	3	75	4	17
18	Graphene/TiO_2	3	128	68	0.39	18
19	LiCl-PEBAX nanofiber	4	30	80	negligible	19
20	CeO_2	3	2-3	9-10	<1	20
21	COF-TXDBA	3	37	42	2.5	This work

References:

1 R. Wang, T. Zhang, Y. He, X. Li, W. Geng, J. Tu and Q. Yuan, *J. Applied Polymer Science*, 2010, **115**, 3474-3480.

2 V. K. Tomer and S. Duhan, *Sens. Actuators B*, 2015, **212**, 517-525.

3 Q. Qi, T. Zhang, X. Zheng and L. Wan, *Sens. Actuators B*, 2008, **135**, 255–261.

4 W. Geng, R. Wang, X. Li, Y. Zou, T. Zhang, J. Tu, Y. He, N. Li, *Sens. Actuators B*, 2007, **127**, 323-329.

5 F. S. Tsai and S. J. Wang, *Sens. Actuators B*, 2014, **193**, 280-287

6 N. Zhang, K. Yu, Z. Zhu and D. Jiang, *Sens. Actuators A*,2008, **143**, 245–250

7 L. L. Wang, H. Y. Wang, W. C. Wang, K. Li, X. C. Wang and X. J. Li, *Sens. Actuators B*, 2013, **177**, 740– 744

8 Y. Qiu and S. Yang, *Adv. Funct. Mater.,*2007,**17**, 1345–1352

9 T. Zhang, R. Wang, W. Geng, X. Li, Q. Qi, Y. He and S. Wang, *Sens. Actuators B*, 2008, **128**, 482-487.

10 M. Anbia and S.E.M. Fard, *Sens. Actuators B*,2011, **160**, 215– 221.

11 R. Sundaram, *Sens. Actuators B*, 2007, **124**, 429–436.

12 S. Hu, H. Chen, G. Fu and F. Meng, *Sens. Actuators B*, 2008, **134**,769–772.

13 N. K Pandey, A. Roy, K. Tiwari, A. Mishra, A. Rai, S. Jayaswal, M. Rashmi and A. Govindan,*1st International Symposium on Physics and Technology of Sensors (ISPTS-1*), *Pune, India,*2012,**1**, 129-132.

14 X. He, W. Geng, B. Zhang, L. Jia, L. Duan and Q. Zhang, *RSC Adv.*, 2016, **6**, 38391

15 Y. Xia, H. Zhao, S. Liu and T. Zhang, *RSC Adv.*, 2014, **4**, 2807

16 Y. Zhen, F.–H. Sun, M. Zhang, K. Jia, L. Li and Q. Xue, *RSC Adv.*, 2016, **6**, 27008

17 T. Fei, H. Zhao, K. Jiang and T. Zhang, *Sens. Actuators B,* 2015, **208**, 277

18 W. –D. Lin ,C.–T. Liao, T.–C. Chang, S.–H. Chen and R.–J. Wu, *Sens. Actuators B*, 2015, **209**, 555

19 S. Liang, X. He, F. Wang, W. Geng, X. Fu, J. Ren and X. Jiang, *Sens. Actuators B*, 2015, **208**, 363

20 V.R. Khadse, S. Thakur, K.R. Patil and P. Patil, *Sens. Actuators B*, 2014, **203**, 229